



HAL
open science

Control strategy with variable commutation instants for MPC based on two flying capacitors connected in parallel

Eduardo Solano, Ana-Maria Llor, Guillaume Gateau, Thierry Meynard, Maurice Fadel

► **To cite this version:**

Eduardo Solano, Ana-Maria Llor, Guillaume Gateau, Thierry Meynard, Maurice Fadel. Control strategy with variable commutation instants for MPC based on two flying capacitors connected in parallel. 2013 15th European Conference on Power Electronics and Applications (EPE), Sep 2013, Lille, France. 9 p., 10.1109/EPE.2013.6634612 . hal-03543486

HAL Id: hal-03543486

<https://ut3-toulouseinp.hal.science/hal-03543486>

Submitted on 26 Jan 2022

HAL is a multi-disciplinary open access archive for the deposit and dissemination of scientific research documents, whether they are published or not. The documents may come from teaching and research institutions in France or abroad, or from public or private research centers.

L'archive ouverte pluridisciplinaire **HAL**, est destinée au dépôt et à la diffusion de documents scientifiques de niveau recherche, publiés ou non, émanant des établissements d'enseignement et de recherche français ou étrangers, des laboratoires publics ou privés.

Control Strategy with Variable Commutation Instants for MPC Based on Two Flying Capacitors Connected in Parallel

E. Solano ^{1,2}, A. Llor ^{1,2}, G. Gateau ^{1,2}, T. Meynard ^{1,2}, M. Fadel ^{1,2}

*Universite de Toulouse ; INPT, UPS; LAPLACE (Laboratoire PLAsma et Conversion d' Energie)
ENSEEIH, 2 rue Charles Camichel, BP 7122, F-31071 Toulouse cedex 7, France
CNRS ; LAPLACE ; F-31071 Toulouse, France*

Keywords

<<Multilevel Converters>>, <<Converter Control>>, <<Digital Control>>, <<Optimal Control>>.

Abstract

In this work we propose a control strategy based on Model Predictive Control (MPC) with variable commutation instants at constant frequency. Two stages are used by association of a reduced cost function and a state machine which selects the optimum state. The strategy is applied to flying capacitor converters connected in parallel, which requires the development of strategies capable to control the external and internal variables of the converter.

Introduction

The introduction of new power converter topologies, able to drive high powers with medium power semiconductor technologies has allowed the fast development of multilevel converters. Nowadays, many different topologies of multilevel converters are possible [1]: Neutral-Point-Clamped (NPC) [2], Flying Capacitor (FC) [3], Cascade H-Bridge converter (CHB) among others. These topologies give a better quality at the output voltage and allow using classical semiconductors and higher dc bus voltages.

On the other hand, the parallel connection of classical topologies, such as regular DC choppers [4] and inverters [5], allows increasing the output currents with the same semiconductor technology. Interleaving techniques can be used in the parallel connection [6] in order to decrease the output current ripple with a fast dynamic response. A magnetic coupling between the output inductors can be carried out in order to decrease the ripple in each output current [7].

In terms of control strategies, the methods used with classical power cells have been extended and used with multilevel converters, as shown in [8]. Most of these strategies are based on classical PWM and use the degrees of freedom generated by additional electronics devices. The most common strategies, presented in [9], include open loop PWM: Sinusoidal PWM (SPWM), Space Vector Modulation (SVM) and Sigma Delta Modulation (SDM). Closed loop PWM using hysteresis or linear control have also been used.

These strategies must ensure a good behavior of the controlled variables and manage all the constraints for each topology. These constraints can be the capacitor voltages in a FC converter or the differential current between two power cells connected in parallel. For more complex topologies, such as multilevel converters connected in parallel, the control strategy may become difficult given the greater number of variables to control.

Predictive control uses the mathematical model and an optimization criterion for selecting the optimal state of the converter. A classification of the different predictive control methods is presented in [10]. The deadbeat control [11] [12] [13] and MPC with finite control set [10] use a modulator in order to generate the required voltage at fixed switching frequency. Hysteresis based [10], trajectory based [14] and Model Predictive Control with finite control set (FS-MPC) [10], use algorithms without modulators and generate directly the switching signals for the converter at variable switching frequency.

The proposed strategy is based on Model Predictive Control (MPC), it uses the converter mathematical model for predicting the future behavior of the controlled variables, for this case the output current i_{mc} , as well as an appropriate criteria such as cost function to select the optimal state. A state machine is used to simplify the selection process of a cost function and also to ensure the respect of all the constraints of the topology.

The power converter topology studied in this paper, used to evaluate the proposed control strategy, is the parallel connection of two 3-level FC (Fig.1). This topology allows increasing the output current, the input voltage and

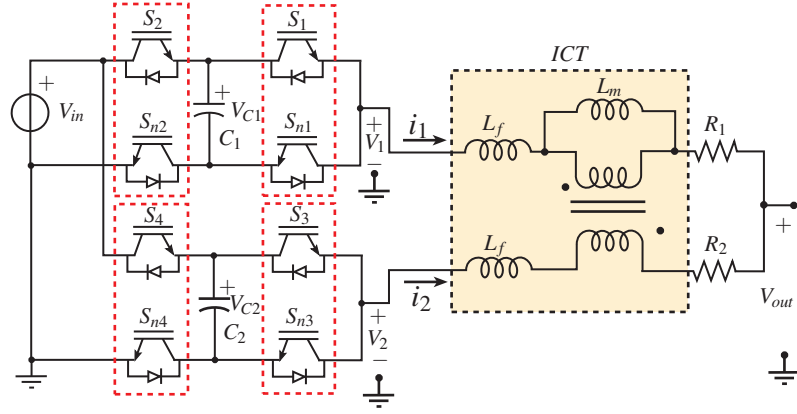


Figure 1: Two FC converters connected in parallel.

the output voltage quality while standard semiconductors are used. The constraints of this topology are related to the capacitor voltages and the differential current. Nevertheless, the control strategy can be easily adapted to other multilevel topologies with a higher number of variables.

Two three-level Flying Capacitors (FC) connected in parallel

Topology

The parallel connection in the studied topology (Fig.1) uses an InterCell Transformer (ICT) but separate inductors can also be used. Each FC contains four switches, the pair of switches S_x and S_{nx} must be always in complementary states. Thus, there are two commutation cells connected in series in each FC: $S_{1,n1}$ and $S_{2,n2}$ for the first FC and $S_{3,n3}$ and $S_{4,n4}$ for the second one. The serial connection is assured by flying capacitors $C_{1,2}$.

The ICT is represented by a classical transformer model, with L_f and L_m representing the leakage and the magnetic inductance. R_1 and R_2 represent the series resistance of each output leg.

Mathematical Model

3-levels FC converter

The series connection of n commutation cells in a FC converter is made via $(n - 1)$ flying capacitors. The output voltage V_{out} contains $(n + 1)$ voltages levels, improving the harmonic spectrum of the output voltage but requiring the voltage balance of each flying capacitor [3] around:

$$V_{Ci} = \frac{i * V_{in}}{n} \quad \text{with} \quad i = 1, \dots, n - 1 \quad (1)$$

The output voltage V_1 and V_2 depend on the input voltage V_{in} and the switch states S_1, S_2, S_3 and S_4 (equation 2). Table I shows the possible switch states for the first FC with the output voltage V_1 and the evolution of the capacitor voltage V_{C1} for an output current i_1 greater than zero.

$$V_{out} = \frac{(S_1 + S_2) * V_{in}}{2} \quad \text{with} \quad S_{1,2} = 1 \text{ if Switch ON and } S_{1,2} = 0 \text{ if Switch OFF} \quad (2)$$

Table I: States of a 3-levels FC converter

State	S_1	S_2	V_{out}	dV_C/dt
1	0	0	0	0
2	0	1	$V_{in}/2$	≥ 0
3	1	0	$V_{in}/2$	≤ 0
4	1	1	V_{in}	0

Parallel connection

The parallel connection of power converters, as previously described, allows an increase of the output current. Nevertheless, a good distribution of this current among the output legs is necessary to assure a good performance of the converter. In [6], it is evidenced that instead of working with phase currents, it is advisable to use a common/differential equivalent circuits. The common mode circuit, representing the equal currents flowing through inductors L_f and the load, is represented in Fig.2.a. The equation 3 describes the equivalent common model circuit (Fig.2.b). This circuit contains an equivalent source $V_{mc} = (V_1 + V_2)/2$ that clarifies the multilevel proprieties of power converters connected in parallel. Two commutation cells having ($n = 2$) output voltage levels, produce a common mode voltage with ($2n - 1 = 3$) levels. The equivalent circuit (Fig.2.b) does not take into account the magnetic coupling of the output inductors.

$$V_{mc} - V_{out} = L_{mc} \frac{d}{dt} i_{mc} + R_{mc} i_{mc} \quad (3)$$

Where: $V_{mc} = (V_1 + V_2)/2$; $i_{mc} = i_1 + i_2$; $L_{mc} = \frac{L_f}{2}$; $R_{mc} = \frac{R_1}{2} = \frac{R_2}{2}$ if $R_1 = R_2$

The differential mode circuit is presented in Fig.2.c, its equivalent circuit is shown in Fig.2.d and described in equation 4. It represents the current flowing through the inductors L_f that it is not flowing through the load. The equivalent source $V_{md} = (V_1 - V_2)/2$ contains also ($2n - 1$) levels. Differential phenomena can entail losses and nonlinearities in the magnetic core, so it is desirable to minimize or cancelate this current.

$$V_{md} = L_{md} \frac{d}{dt} i_{md} + R_{md} i_{md} \quad (4)$$

Where: $V_{md} = \frac{V_1 - V_2}{2}$; $i_{md} = i_1 - i_2$; $L_{md} = L_f$; $R_{md} = R_1 = R_2$

Studied topology

The parallel connection of two 3-levels FC ($n = 3$), contains 4 commutation cells ($S_{1,n1}, S_{2,n2}, S_{3,n3}, S_{4,n4}$) and thus, $2^4 = 16$ states. The V_{mc} voltage produces ($2n - 1 = 5$) levels: $[0, E/4, E/2, 3E/4, E]$ while the V_{md} voltage produces the voltage levels: $[-E/2, -E/4, 0, E/4, E/2]$. Table II shows all the states of this topology, the V_{mc} , V_{md} and the variations of each capacitor voltage V_{C1} and V_{C2} for $i_{1,2}$ greater than zero.

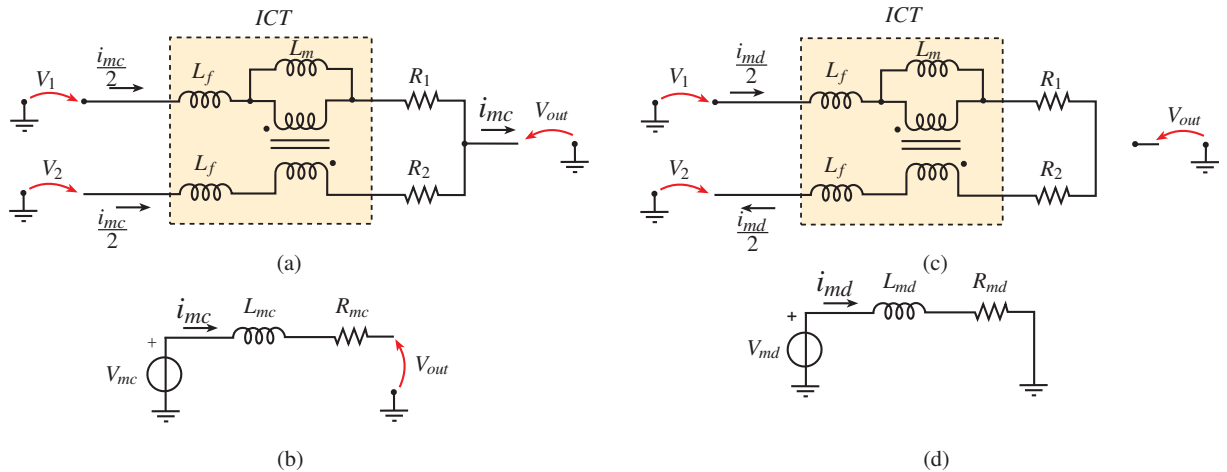


Figure 2: (a) Common mode circuit (b) Equivalent common mode circuit (c) Differential mode circuit (d) Equivalent differential mode circuit

Predictive Control

MPC has been widely employed in research and industrial control systems given its intuitive concept and the ability to account for nonlinearities or multivariable cases. Its uses the mathematical model and an optimization criterion for selecting the optimal state of the converter and it has already been applied for controlling multilevel converters, such as NPC [15] and FC [16]. Figure 3(a) shows the scheme for controlling a power converter with n switches. The variables to be controlled ($V_{C1,C2}$, i_{mc} and i_{md}) are measured at each sampling instant k . The forward Euler approximation can be used to get the discrete system model and thus, to predict the behavior of the variables for all the states at the $k + 1$ instants. This information is used by the controller for obtaining the optimal actuation

Table II: States of two 3-level FC converters connected in parallel

State	S_1	S_2	S_3	S_4	V_{mc}	V_{md}	dV_{C1}/dt	dV_{C2}/dt
1	0	0	0	0	0	0	0	0
2	1	0	0	0	$E/4$	$E/4$	≤ 0	0
3	0	1	0	0	$E/4$	$E/4$	≥ 0	0
4	1	1	0	0	$E/2$	$E/2$	0	0
5	0	0	1	0	$E/4$	$-E/4$	0	≤ 0
6	1	0	1	0	$E/2$	0	≤ 0	≤ 0
7	0	1	1	0	$E/2$	0	≥ 0	≤ 0
8	1	1	1	0	$3E/4$	$E/4$	0	≤ 0
9	0	0	0	1	$E/4$	$-E/4$	0	≥ 0
10	1	0	0	1	$E/2$	0	≤ 0	≥ 0
11	0	1	0	1	$E/2$	0	≥ 0	≥ 0
12	1	1	0	1	$3E/4$	$E/4$	0	≥ 0
13	0	0	1	1	$E/2$	$-E/2$	0	0
14	1	0	1	1	$3E/4$	$-E/4$	≤ 0	0
15	0	1	1	1	$3E/4$	$-E/4$	≥ 0	0
16	1	1	1	1	E	0	0	0

according to a predefined optimization criterion, expressed usually as a cost function g .

Several compositions of the cost function have been proposed depending on the system and control requirements, equation 5 shows the simplest choice when several variables have to be controlled. Each term includes the difference between the reference variable and the predicted value at $(k+1)$ instants, weighting factors (α , β , δ) are also included for offsetting the difference of the variables nature and also for fixing some priorities. Other terms representing some specific request, such as limitation of the switching commutation, can be included.

$$g = \alpha |i_{mc}^*(k+1) - i_{mc}(k+1)| + \beta |i_{md}^*(k+1) - i_{md}(k+1)| + \delta |V_{C1,C2}^*(k+1) - V_{C1,C2}(k+1)| \quad (5)$$

However, when the number of variables increases, the calculation of the weighting factors in the cost function can become a straightforward task. An algorithm using a certain number of simulations to get the appropriate weighting factors in a particular operational point is presented in [17].

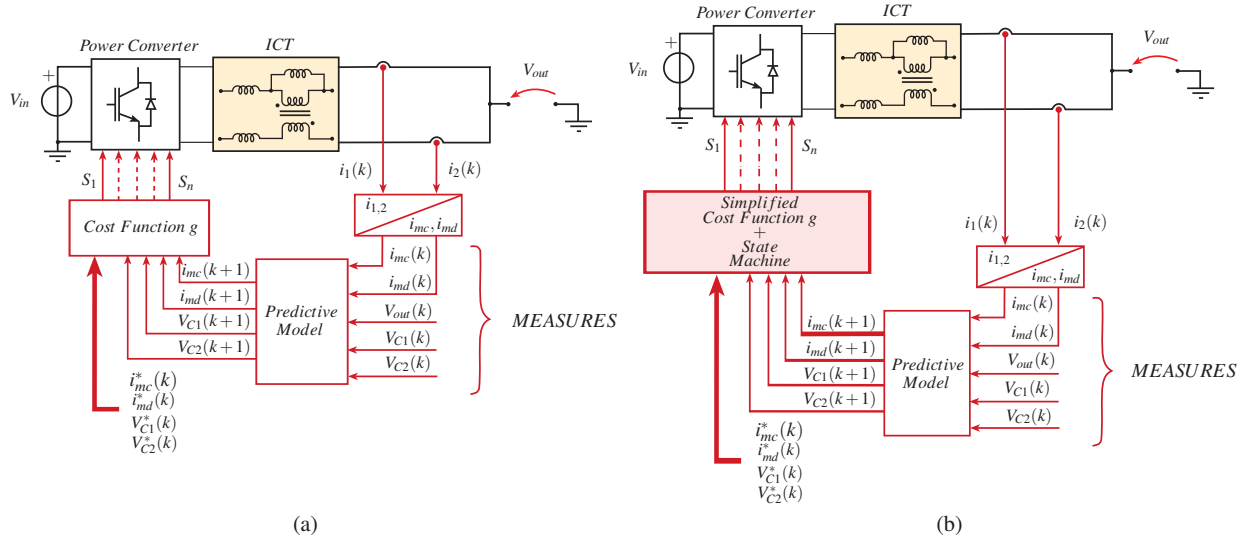


Figure 3: (a) Classical MPC strategy (b) Proposed MPC control strategy

Proposed control strategy

The first part of the control strategy is based on MPC for controlling the common mode current (i_{mc}). A new idea concerning a variable commutation instant is added to improve the behavior of the controlled variable. This variation of the classical strategies with fixed commutations not only allows choosing the best voltage level to commute but also the best instant to make the commutation in order to get the desired voltage. So, there are two

variables to be calculated at each sampling period (T_s). The first one is the commutation instant (t_k) and the second one is the predicted value ($i_{mc}(k+1)$) for the next calculation step.

Calculations are based on the predictive model, the measures taken at each sampled time and the possible variation of the mode common voltage V_{mc} . For the studied topology, these variations are:

- $\Delta V_{mc} = +E/4$ if $S_j = 1$ with $j = 1, 2, 3, 4$.
- $\Delta V_{mc} = -E/4$ if $S_j = 0$ with $j = 1, 2, 3, 4$.
- $\Delta V_{mc} = 0$ if there is no commutation.

Calculation of t_k and $i_{mc}(k+1)$ are obtained from the equations 5 and 6 after discretization. Fig. 4(b) shows the principle of the control strategy. With the measures at the k instant, the $i_{mc}(k+1)$ current at the t_k instant can be calculated:

$$i_{mc}(t_k) = \frac{t_k}{L_{mc}} (V_{mc}(k) - V_{out}(k)) + i_{mc}(k) \quad (6)$$

Between $t_k \leq T_s$, the V_{mc} voltage may change ΔV_{mc} , so the current i_{mc} at $k+1$ is:

$$i_{mc}(k+1) = \frac{(T_s - t_k)}{L_{mc}} * (V_{mc}(k) - V_{out}(k) + \Delta V_{mc}(t_k)) + i_{mc}(t_k) \quad (7)$$

For simplicity, it is considered that the reference current i_{mc}^* does not change in one sampling interval, so $i_{mc}^*(k+1)$ is equal to $i_{mc}^*(k)$.

$$t_k = \frac{T_s}{\Delta V_{mc}(t_k)} * (V_{mc}(k) - V_{out}(k) + \Delta V_{mc}(t_k)) - \frac{L_{mc}}{\Delta V_{mc}(t_k)} * \varepsilon_{i_{mc}}(k) \quad (8)$$

Where: $\varepsilon_{i_{mc}}(k) = |i_{mc}^*(k+1) - i_{mc}(k)|$

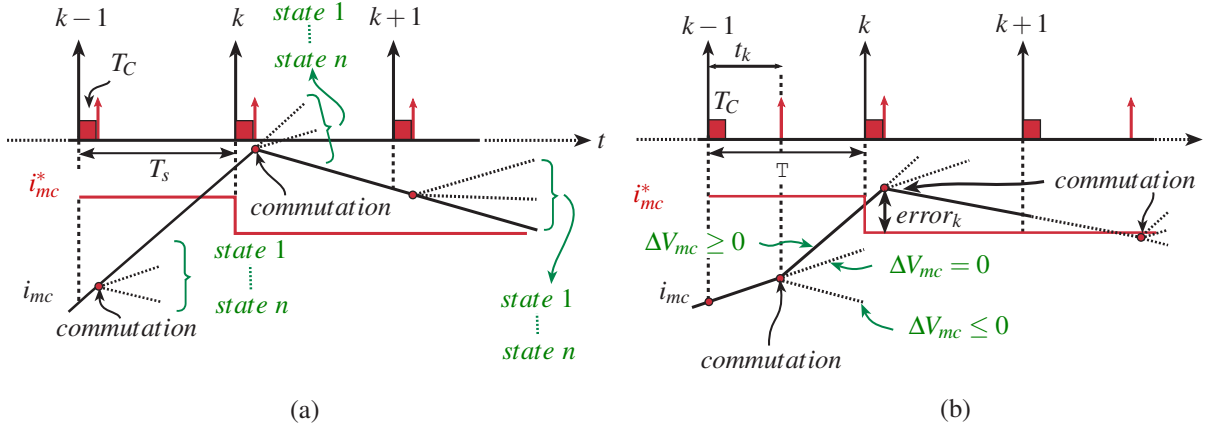


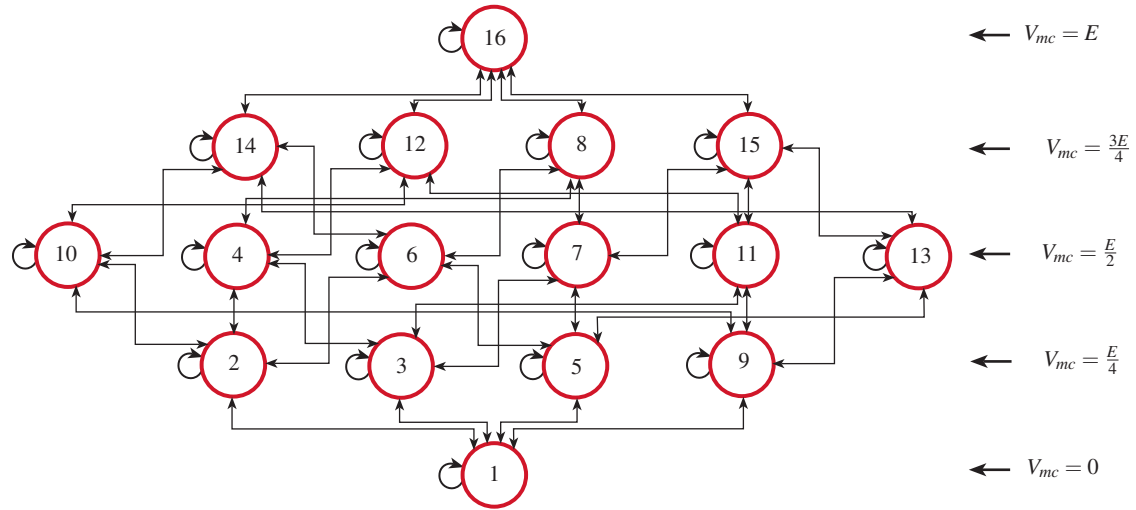
Figure 4: (a) Commutations in classical MPC strategy (b) Commutations in proposed control strategy

The three values of the commutation instant t_k (each one calculated for a different ΔV_{mc}) are limited between the calculation time (T_C) and the sampling period (T_s). Thereafter, the calculation of $i_{mc}(k+1)$ can be obtained from equation 7.

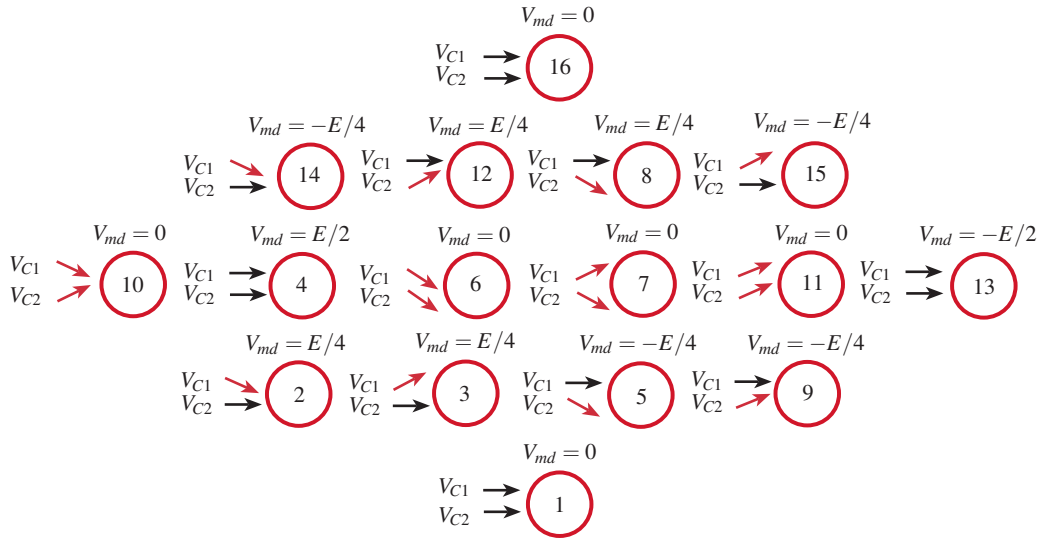
Three predicted values of $i_{mc}(k+1)$ are obtained and the optimization criterion g is then applied. This criteria is the minimization of the error $g = |i_{mc}^*(k+1) - i_{mc}(k+1)|$ at instant ($k+1$). The optimal values of t_k and ΔV_{mc} are then found.

Fig. 5(a) represents the state machine used for the second part of the control strategy. In this state machine, the 16 states of the studied topology have been arranged and each row represents the same V_{mc} voltage level. The possible transitions between certain states are limited by the number of commutations. Therefore, one commutation of one commutation cell for each calculation period will be respected.

Fig. 5(b) shows the variations of V_{mc} , V_{md} , V_{C1} and V_{C2} for each state, when the output current I_{mc} is positive.



(a)



(b)

Figure 5: (a) State machine for two flying capacitors connected in parallel and the possible transitions between the different states. (b) Variation of V_{md} , V_{C1} and V_{C2} for each state for a output current greater than zero.

Control of the differential current i_{md}

The differential current is indirectly controlled via the time spent in each state that increases or reduces this current. When the ΔV_{mc} is selected, the chosen state of the next level voltage will be the one that can take the current closest to zero at the end of the sampling time. That means that the reference value for the differential current is $i_{md}^* = 0$. In order to reduce the fast variations of i_{md} , states 4 and 13 which produce a high value of V_{md} are forbidden.

The amplitude of the differential current is related to the possible saturation of the magnetic core used in the ICT. This is because the differential current represents a dc magnetic flux into the magnetic core, which can impose an operation point close to the saturation zone.

So, the amplitude of this current must be limited, principally during transients. A prediction of current i_{md} at the instant $(k + 1)$ will be made. If the current exceeds the established limits, a dynamic action is necessary to restore the value of i_{md} around zero. Strategies such as a reduction of the commutation instant t_k or the execution of a double commutation (two cells commutate at the same time) producing a higher slope in the i_{mc} dynamics, can be used.

Control of the Capacitor Voltages V_{C1} and V_{C2}

The supervision of each flying capacitor voltage follows the same principle that the differential current control with a lower priority. Thus, when the states respecting the V_{mc} and the V_{md} required have been selected, the selection of the next state will be made according to the voltage evolution required for each capacitor.

Let's see these steps through an example:

Let's say that the state at the k instant is 1. Currents and flying voltages measures are made and t_k is calculated with equation 6. Let's suppose that ΔV_{mc} to be applied at t_k is greater than zero.

Fig. 5 shows that there are four possible states to commutate: 2, 3, 5 and 9. States 2 and 3 produce a differential voltage greater than zero while states 5 and 9 produce a negative differential voltage.

If the differential current i_{md} at the instant k is greater than zero, there are two possible states for decreasing this current at the next commutation: states 5 and 9. For these two states V_{C1} will not change but V_{C2} rise in the state 9 and decrease in state 5. So, if the measured value of V_{C2} is greater than $E/2$, the next state will be 5. If the value of this capacitor voltage is lower than $E/2$, the next state will be 9.

Simulation and results

The proposed strategy was implanted with PSIM. The simulation parameters have been chosen according the experimental setup that is actually being carried out. These parameters are: $V_{in} = 100[V]$, $L_f = 6[mH]$, $L_m = 60[mH]$, $T_s = 50[\mu s]$, $C_{1,2} = 100[\mu F]$, $R_{1,2} = 250[m\Omega]$, $R_l = 12[\Omega]$.

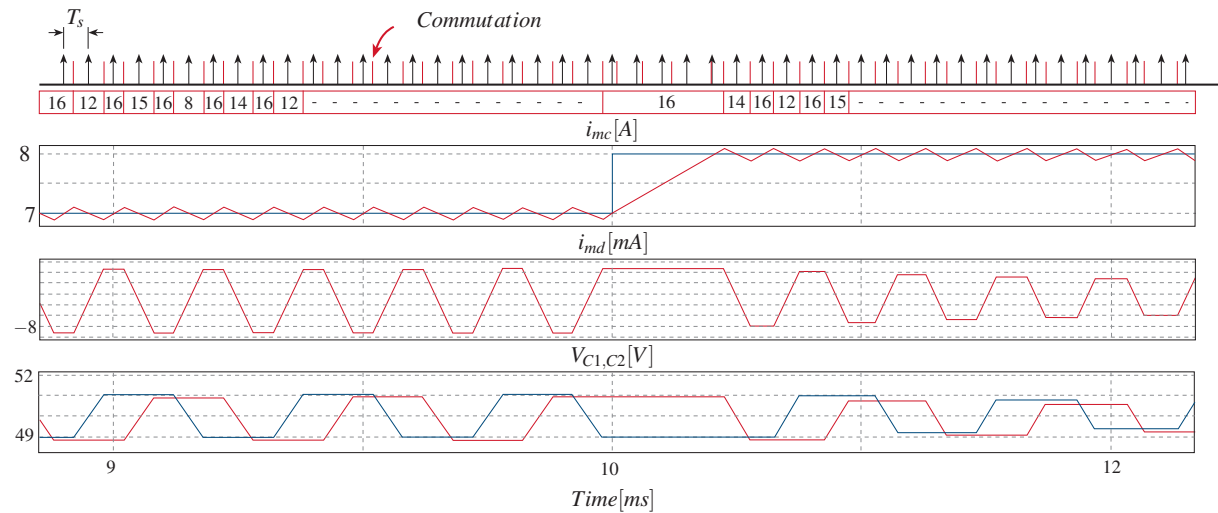


Figure 6: Simulations results for the proposed strategy

Fig. 6 shows the simulation results when the current reference is fixed at 7[A] with a perturbation of 1[A] at $t = 10[ms]$. One commutation is executed in each sample time for a steady state operation, the control of the I_{mc} current is thus guaranteed between the states with a V_{mc} equal to $3E/4[V]$ and $E[V]$. The differential current and the capacitor voltages are controlled with an appropriate transitions for the states 14, 12, 8 and 15.

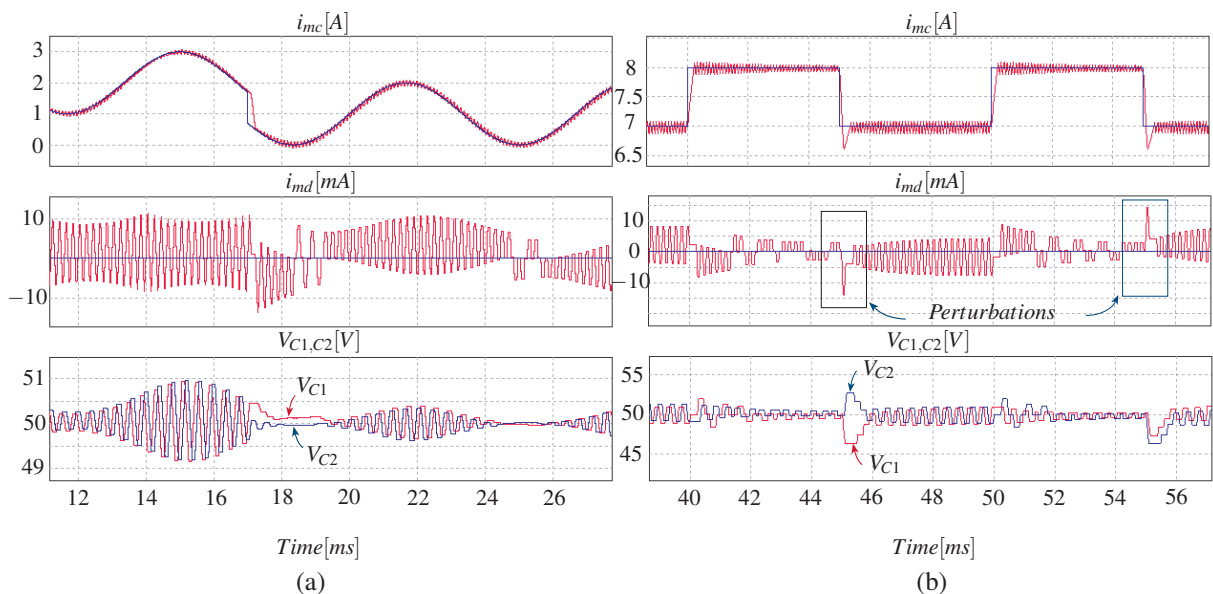


Figure 7: Perturbation of the reference current I_{mc}^* for a (a) sinusoidal waveform and (b) squared waveform

In terms of dynamic behavior, the proposed strategy presents the same advantages of the classical MPC: a fast response of the controlled variable. During the transients, the commutation are performed at the final of the calculation time (T_c) fixed in these simulations at $10[\mu s]$.

Fig. 7 shows the transient response with the control strategy for a sinusoidal (a) and a square (b) current references.

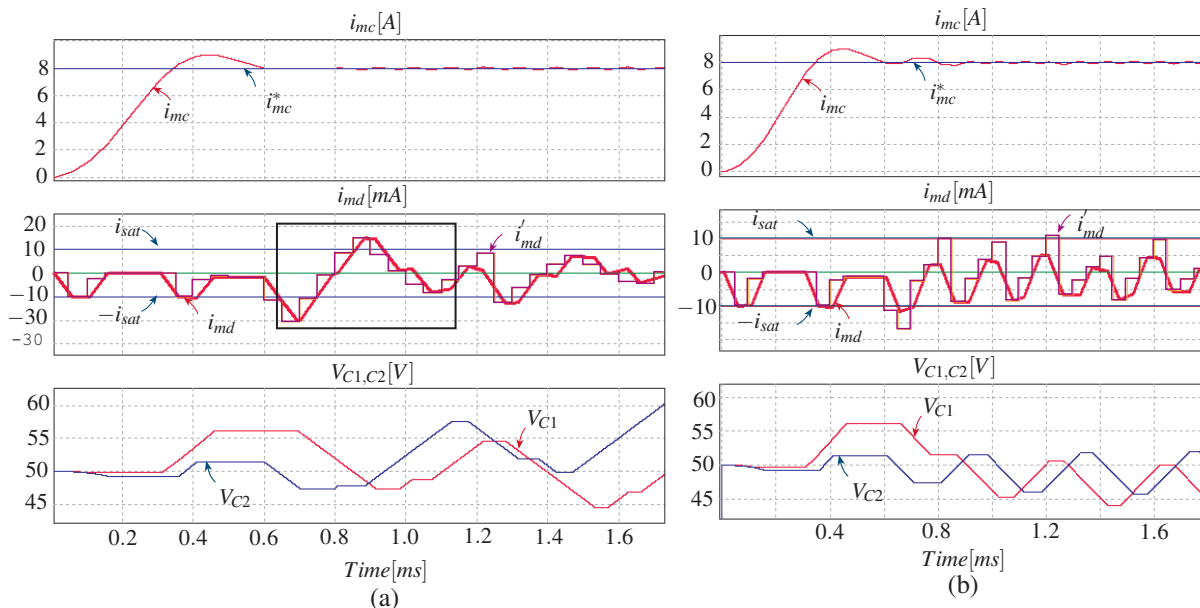


Figure 8: (a) Perturbation of the differential current i_{md} (b) Reduction of the differential current i_{md} oscillations

In some cases, high variations of the reference current i_{mc}^* can produce important perturbations in the differential current i_{md} . In order to avoid non linear and saturation phenomena in the magnetic core, a survey of i_{md} (based on equation 4) for each sample time is made, this survey will avoid the perturbations of the differential current beyond the establish value ($\pm i_{sat}$). Fig. 8(a) gives an example of this problem, a recalculation of the commutation instants (t_k) is presented here when the calculated i_{md} reaches the i_{sat} value. When the commutation is applied at the new t_k , the oscillations of the differential current are reduced (Fig. 8(b)). Another solution for reducing the i_{md} perturbations, consists in the execution of a double commutation (two cells commute at the same time) when i_{md} exceeds $\pm i_{sat}$.

Conclusion

In this paper, it is presented a new strategy based in MPC with variable commutation instants. The most important differences of the proposed strategy with the classical MPC are the variation of the commutation instants in each sampled period, the use of a constant switching frequency and the use of a simplified cost function with a state machine. The goal of using variable commutation instants is to reduce the error of the controlled variables at the end of the sampling period, thus not only the necessary voltage level is applied, but also the commutation instant is appropriately placed for minimizing the output current error at the end of each simple period. The simplified cost function allows a reduction of the calculations compared with traditional MPC, the state machine allows a better selection of the optimal state in order to manage the internal variables of the converter.

This strategy is used in two flying capacitors connected in parallel, but it can be applied in topologies with a high number of variables and parameters to be controlled, such as new multilevel series and parallel converters.

The principal variable to be controlled is included in the optimization criterion to be minimized at each sampling time while the other variables are controlled by the transitions in a state machine containing all the possible switch states.

The required survey of certain variables (such as I_{md} in the parallel connection) can be done by a prediction of this variable in each sampling time. Some double commutations can be a solution when some redundancies in the system are present.

References

- [1] L. Franquelo, J. Rodriguez, J. Leon, S. Kouro, R. Portillo, and M. Prats, "The age of multilevel converters arrives," *IEEE Industrial Electronics Magazine*, vol. 2, pp. 28–39, June 2008.
- [2] A. Nabae, I. Takahashi, and H. Akagi, "A new neutral-point-clamped PWM inverter," *IEEE Transactions on Industry Applications*, vol. IA-17, pp. 518–523, Sept. 1981.

- [3] T. Meynard and H. Foch, "Multi-level conversion: high voltage choppers and voltage-source inverters," in , *23rd Annual IEEE Power Electronics Specialists Conference, 1992. PESC '92 Record*, pp. 397–403 vol.1, July 1992.
- [4] J. Li, C. Sullivan, and A. Schultz, "Coupled-inductor design optimization for fast-response low-voltage DC-DC converters," in *Seventeenth Annual IEEE Applied Power Electronics Conference and Exposition, 2002. APEC 2002*, vol. 2, pp. 817–823 vol.2, 2002.
- [5] C. Liangliang, X. Lan, H. Wenbin, and Y. Yangguang, "Application of coupled inductors in parallel inverter system," in *Sixth International Conference on Electrical Machines and Systems, 2003. ICEMS 2003*, vol. 1, pp. 398–401 vol.1, Nov. 2003.
- [6] B. Cougo, G. Gateau, T. Meynard, M. Bobrowska-Rafal, and M. Cousineau, "PD modulation scheme for three-phase parallel multilevel inverters," *IEEE Transactions on Industrial Electronics*, vol. 59, pp. 690–700, Feb. 2012.
- [7] P.-L. Wong, P. Xu, P. Yang, and F. Lee, "Performance improvements of interleaving VRMs with coupling inductors," *IEEE Transactions on Power Electronics*, vol. 16, pp. 499–507, July 2001.
- [8] Colak I., Kabalci E., and Bayindir R., "Review of multilevel voltage source inverter topologies and control schemes," *Energy Conversion and Management*, vol. 52, pp. 1114–1128, Feb. 2011.
- [9] J. Holtz, "Pulsewidth modulation for electronic power conversion," *Proceedings of the IEEE*, vol. 82, pp. 1194–1214, Aug. 1994.
- [10] P. Cortes, M. Kazmierkowski, R. Kennel, D. Quevedo, and J. Rodriguez, "Predictive control in power electronics and drives," *IEEE Transactions on Industrial Electronics*, vol. 55, pp. 4312–4324, Dec. 2008.
- [11] O. Kukrer, "Discrete-time current control of voltage-fed three-phase PWM inverters," pp. 260–269, Mar. 1996.
- [12] Q. Zeng and L. Chang, "An advanced SVPWM-Based predictive current controller for three-phase inverters in distributed generation systems," pp. 1235–1246, Mar. 2008.
- [13] W. Stefanutti, E. Tedeschi, P. Mattavelli, and S. Saggini, "Digital deadbeat control tuning for dc-dc converters using error correlation," pp. 1–6, June 2006.
- [14] M. Depenbrock, "Direct self-control (DSC) of inverter-fed induction machine," pp. 420–429, Oct. 1988.
- [15] R. Vargas, P. Cortes, U. Ammann, J. Rodriguez, and J. Pontt, "Predictive control of a three-phase neutral-point-clamped inverter," *IEEE Transactions on Industrial Electronics*, vol. 54, pp. 2697–2705, Oct. 2007.
- [16] E. Silva, B. McGrath, D. Quevedo, and G. Goodwin, "Predictive control of a flying capacitor converter," in *American Control Conference, 2007. ACC '07*, pp. 3763–3768, July 2007.
- [17] J. Rodriguez and P. Cortes, *Predictive Control of Power Converters and Electrical Drives*. WILEY, Apr. 2012.